Performance of an optical sectored receiver for indoor wireless communication systems in presence of artificial and natural noise sources

António M. R. Tavares, Rui J. M. T. Valadas, A. M. de Oliveira Duarte

Integrated Broadband Communications Group, Dept. of Electronics and Telecommunications
University of Aveiro, 3810 AVEIRO, PORTUGAL

ABSTRACT

This paper gives special attention to wireless local area networks using infrared technology mainly with respect to the reception techniques and will present the performance evaluation of optical sectored receivers for indoor wireless communication systems in presence of artificial and natural noise sources. Performance evaluation was extended to four distinct sectored receiver configurations which result in significant gains over a non-sectored optical receiver.

A characterisation of the ambient light noise distribution due artificial light was performed. Also, the radiation patterns of some directional incandescent lamps were measured and modelled through a generalised Lambertian function. The feasibility of optical sectored receivers in presence of directional light sources was demonstrated.

Keywords: wireless, infrared communication systems, diffuse infrared channel, optical sectored receiver, spot lamps

1. INTRODUCTION

Wireless indoor infrared (IR) communication systems were initially proposed by Gfeller[1]. Since then many contributions[2-10] have been presented. The increase of systems baud rate and communication range are pushing the utilisation of new network topologies, new emission and receiver methods and new techniques to combat optical noise and multipath dispersion.

A property of electromagnetic radiation which is also applicable to indoor IR communication systems is interference due to multipath dispersion. Multipath dispersion can be significant in indoor IR systems producing high levels of intersymbol interference. Therefore, multipath dispersion must be considered in the design of wireless IR systems with baud rates higher than a few MHz[5,9]. Wireless indoor IR communication systems occupy an electromagnetic spectrum window which is also shared by sun light and artificial light. Natural and artificial light sources produce a large quantity of IR radiation which induces a large amount of optical noise in the receiver, limiting its sensitivity. Moreover, the proximity between near infrared and visible light turns its main propagation properties similar: i) high absorption level of dark materials, ii) high reflection level produced by bright materials and iii) existence of a large quantity of opaque materials which can block the infrared radiation producing a shadow area. As the radiation wavelength is smaller, comparatively to the physical dimensions of usual objects, there is a small amount of refraction but a high quantity of reflection. The reflection pattern has, usually, two components: i) specular (originated by smooth surfaces) and, ii) diffuse (originated by rough surfaces).

Usually, receivers for IR communication systems are based on a single optical detector. This may be a good configuration in environments where both, signal and noise are isotropic. However, in most environments the transmitted signal illuminates the receiver from privileged directions. Also, the ambient light noise emanates from particular directions coinciding with the position of lamps or windows. Moreover, the light noise sources are, usually, in the receiver field-of-view (FOV). These particularities enlarge the dynamic range of the Signal to Noise Ratio (SNR) which depends significantly from the receiver orientation.

To minimise the effects of SNR fluctuations, two new receiver techniques were recently proposed[2,7]. Gfeller[7] proposed a new receiver technique to combat the spatial and temporal changes of the ambient optical noise. The proposed method adjusts the data rate, maintaining full network capability. Another new technique to minimise ambient light noise effects was proposed by Valadas[2]. The proposed technique exploits the directional nature of both signal and noise through the use of diversity techniques. This solution is based on an optical sectored receiver which presents significant gains in reducing the penalty induced by ambient noise. Sectored receivers may also be used in combating multipath dispersion[6] of the indoor optical channel.

 0-8194-1965-6/95/$6.00

An IR sectored receiver can be defined by a set of optical receivers (sectors) with a relative small FOV. Each sector estimates the SNR of the collected signal. The gain of a sector is proportional to the relation i/σ^2, where i and σ represent the average signal and the *rms* shot noise, respectively. In the case of a maximal-ratio combining receiver, the output signals are weighted and added. Alternately, the output of the sector with the best SNR (Best-sector selection receiver), can be considered.

In this paper we evaluate the performance gains of maximal-ratio sectored receivers in combating ambient light noise. Section 2 presents the signal propagation models. In section 3, a set of measurements of the optical noise distribution is presented and a radiation model of the spot lamps is proposed. Performance evaluation of sectored receivers is addressed in section 4. Finally, section 5 presents the main conclusions of this work.

2. PROPAGATION MODELS

In this paper we limit our study to empty rectangular rooms. The signal propagation model includes the emitter model, the reflector model and the sectored receiver model.

2.1. Emitter model

We model the optical emitter using a generalised Lambertian source. According this model, the angular distribution of the emitter radiant intensity is:

$$E(\theta) = P_S \frac{n+1}{2\pi} \cos^n(\theta) \tag{1}$$

where P_S represent the total power emitted power and θ is the angle from the normal to the emitting surface. The angular spread of the beam is defined by n which is given by $n = \ln(1/2)/\ln(\cos hpa)$ where hpa is the half-power angle of the emitter.

2.2. Reflector model

The considered reflection model assumes that the ceiling surface was a purely diffuse Lambertian surface. In such model the power emitted by a differential element of the surface is independent of the angle of incident radius. The ratio of the power transmitted by each differential element is called reflection coefficient (ρ) and in our case it was assumed unitary.

2.3. Sectored receiver model

In our work we used the sectored receiver model proposed by Valadas[2]. The sectored receiver is assumed to be a hemisphere where a set of parallels and equal spaced meridians define the boundaries of the sectors. The region of the sectored receiver between to parallels is called a segment. Each sector is completely defined through its active area and Field-of-View. The *FOV* of a sector is specified by the two limiting elevation angles, θ_h and θ_l, and the two limiting azimuth angles, φ_h and φ_l, where $\theta_h \geq \theta_l$ and $\varphi_h \geq \varphi_l$. The used sectored receiver model considers an unitary area hemisphere. The orientation of each sector is defined as $\theta_{Rs} = (\theta_h + \theta_l)/2$ and $\varphi_{Rs} = (\varphi_h + \varphi_l)/2$ except in the case of a polar sector where $\theta_{Rs} = 0$ (sectored pointed vertically).

A sectored receiver can be completely specified through a set Ψ with a subset for each segment as represented in (2).

$$\Psi = \{\{N_{S1}, \varphi_{01}, \theta_{l1}, \theta_{h1}\}, \{N_{S2}, \varphi_{02}, \theta_{l2}, \theta_{h2}\}, \ldots, \{N_{Sn}, \varphi_{0n}, \theta_{ln}, \theta_{hn}\}\} \tag{2}$$

Each subset characterise a segment and has four elements specifying: i) the number of sectors N_S, ii) the azimuth off-set of the first sector φ_0 and iii) the limiting elevation angles θ_h and θ_l. All sectors belonging to the same segment have an equal azimuth aperture, $360^o/N_S$. This sectored receiver model[2] assures that there is no overlap between the reflecting surfaces seen by each sector.

An example of a sectored receiver is represented in Fig. 1. This sector has 2 segments with a total of 9 sectors.

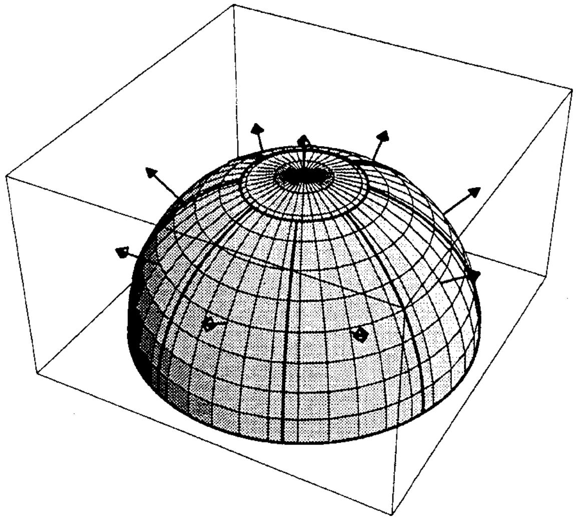

Figure 1. Sector receiver with 2 segments and 9 sectors:
$\Psi = \{\{1, 0^{o}, 0^{o}, 20^{o}\}, \{8, 22.5^{o}, 20^{o}, 90^{o}\}\}$

3. AMBIENT LIGHT NOISE

Ambient light noise may vary over several decades[10] during a day in a typical office environment. IR communication systems are exposed to two classes of ambient light noise: i) natural light (sun light) and ii) artificial light. Artificial light can be divided in two subsets depending of its origin (incandescent or fluorescent). These light sources induce shot noise into the optical receiver. Both, artificial light produced by incandescent lamps and natural light are infrared sources and its amplitudes change slowly with the time. In this case, induced shot noise can be largely reduced through the utilisation of high-pass or band-pass optical filters. On the other side, the artificial light which comes from fluorescent lamps has an intensity modulated characteristic. This modulation can be performed at the mains power frequency or, through the use of electronic ballasts, this modulation can be made up to hundreds of kHz. The optical interference due to such lamps can have significant harmonics up to 1MHz[8]. Optical filtering can reduce significantly the amplitude of this interference. However, it is mandatory to use adequate electrical filtering. Even using all these filtering techniques, the SNR could have significant fluctuations depending mainly of the spatial shot noise distribution within the communication cell.

3.1. Spatial shot noise distribution

In order to characterise the artificial optical noise distribution within an office room, we made some measurements of the spatial ambient light noise distribution in two different test rooms. The illumination in these test rooms were produced by two extreme cases: i) fluorescent lamps, ii) directional incandescent lamps (also called spot lamps). A brief description of each test room and measurement setup is provided here:

Test room 1: This is a rectangular-shaped laboratory dark room. This test room is empty and is illuminated by 8 (4 × 2) fluorescent lamps of *36 W*. Test room 1 has no windows and has the following dimensions: *6.0 m* × *4.5 m* × *3.1 m* (*Length* × *Width* × *Height*). Test room layout and relative position of fluorescent lamps are shown in figure 2a.

Test room 2: This is a rectangular-shaped meeting room with 4 large tables, several chairs and large curtained windows on the east side. Test room dimensions are: *7.0 m* × *5.0 m* × *2.6 m* (*L* × *W* × *H*). The illumination of this room is composed by 9 spot lamps of *100 W*. The measurements in this test room were performed at night to neglect the contribution of natural light which emanates from windows. Test room layout and relative position of spot lamps are shown in figure 2b.

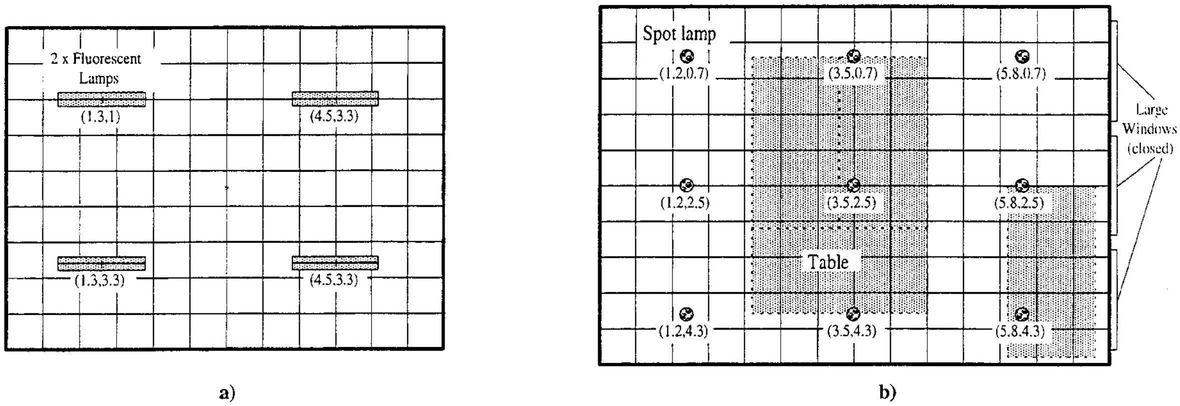

Figure 2. General layout for a) test room 1 and b) test room 2

Measurement setup: The measurements of the ambient light noise were performed through the measurement of the *DC* photocurrent induced in a PIN photodiode vertically oriented and pointed straight up. The measurement setup was located *0.96 m* above the floor. The used PIN photodiode has the following characteristics: i) an active area of *0.85* cm^2, ii) a parasitic capacitance of *120 pF* (with a reverse voltage across the photodiode of *15 V*), iii) a field of view of *85°*, and iv) a responsitivity of *0.6 A/W* at a centre wavelength of *850 nm*.

The spatial distribution of the optical noise induced by fluorescent and directional incandescent lamps was measured with a resolution of *0.5 m*. The measured values were fitted linearly to surfaces with *0.5 m* grid size and are represented in figures 3a and 3b.

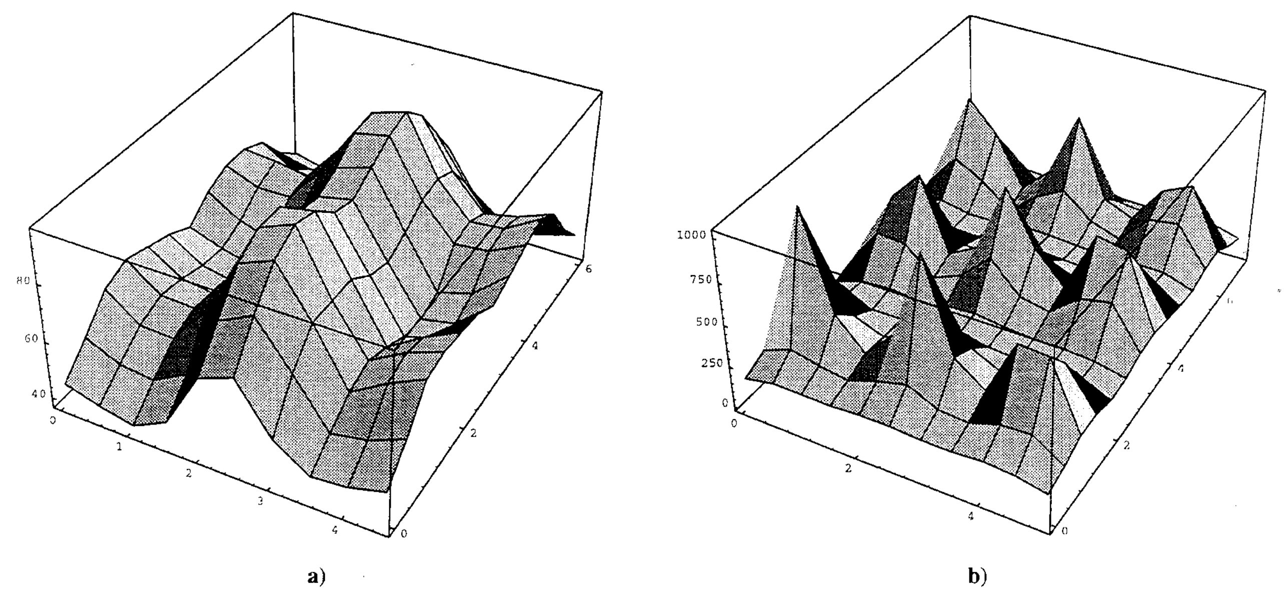

Figure 3. Spatial distribution of DC currents induced in the photodiode **a)** test room 1 and **b)** test room 2.

The maximum and minimum values measured within the test room 1 were *96.9* $\mu A/cm^2$ and *37.8* $\mu A/cm^2$, respectively, which results in a dynamic range of about *4.09 dB*. On the other side, in test room 2, the dynamic range of the optical noise distribution produced by spot lamps was about *8.56 dB*. The maximum and minimum values measured were *1020* $\mu A/cm^2$ and *142* $\mu A/cm^2$.

These results show that the ambient optical noise has a strong spatial dependence and that the optical noise can be more intense under spot lamps. This effect was also observed by Gfeller[7] which denominated the maximum shot noise points under incandescent desk lamps as "hole burning effect".

It seems obvious that the large dynamic range of shot noise spatial distribution produced by spot lamps together with the large dynamic range of the signal will produce a correspondent large dynamic range in the SNR within an infrared communication cell. More, the utilisation of spot lamps has been generalised, mainly in conference and meeting rooms and spot lamps have, usually, a relative narrow radiation pattern. So, it is important to study the performance of sectored receivers in a such hostile environment as the verified in test room 2. Thus, it will be necessary to characterise the radiation pattern of spot lamps.

3.2. Spot lamp radiation pattern: characterisation and modelling

In order to characterise and model the radiation pattern of spot lamps, a large set of measurements was performed. This measurements were extended to seven distinct spot lamps which are usually utilised in meeting rooms, conference rooms, etc. Table 1 presents the characterised spot lamps. Spot lamp A is identical to the 9 spot lamps used to illuminate test room 1.

Spot Lamp	Reference
A	OSRAM, CONCENTRA SPC, R95, 100W
B	TUNGSRAM, TUNGRAFLEX, KBL, R95, 100W
C	SPLENDOR, REFLECTORLAMP, R95, 75W
D	SPLENDOR, SP, R80, 75W
E	PHILIPS, SUPERPHILUX, R80, 100W
F	PHILIPS, REFLECTOR, R95, 150W
G	PHILIPS, SPOTLINE, R80, 100W

Table 1. Identification of the characterised spot lamps.

The measurements were performed in the dark room previously identified as test room 1. Spot lamps were placed in the centre of the ceiling and were oriented to the floor. Measurement setup was identical to the setup used in section 3.1 and was placed at *10 cm* above the floor with the photodiode straight up oriented. Measurements were made along four axes (longitudinal, transversal and diagonal) centred on the illumination pattern from the spot lamps. Figure 4 illustrates the normalised power distribution as a function of distance from the centre of each spot lamp radiation pattern.

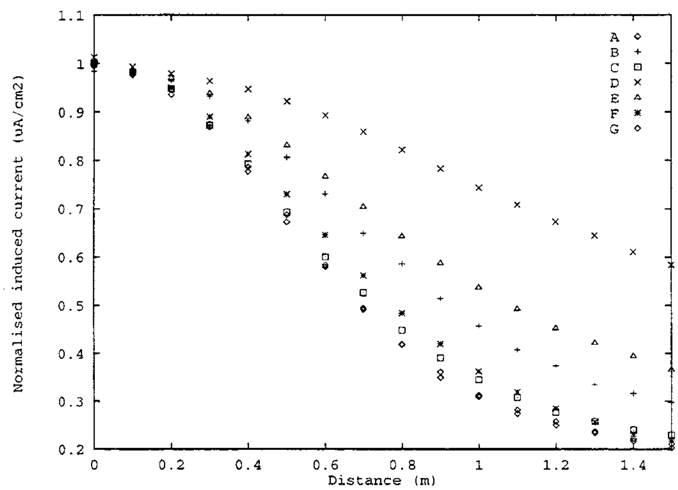

Figure 4. Normalised power distribution versus distance.

From an intuitive analysis of figure 4, we attempted to model the radiation pattern of spot lamps as a generalised Lambertian function. This procedure was realised by a non-linear fit of the measured values to the function (2) which characterise the optical power received from a Lambertian source when the emitter is straight down oriented and the receiver is straight up oriented.

$$P_R(x) = A \cos\left[\arctan\left(\frac{x}{h}\right)\right]^{n+3} \tag{2}$$

where h is the distance from the ceiling to the photodiode, A is a parameter proportional to the transmitted power and n is the parameter which defines the angular spread of the beam. The results obtained through the fitting of measured values are presented in table 2. The accuracy of the fitting curve is defined by a fitting error parameter. This parameter is the maximum value of the difference between each measured and the fitting curve values normalised to the measured value.

Spot Lamp	n	hpa	fitting error
A	*32.79*	*11.74*	*2.2%*
B	*19.20*	*15.30*	*2.7%*
C	*32.58*	*11.78*	*2.3%*
D	*6.89*	*25.27*	*1.3%*
E	*17.39*	*16.07*	*1.0%*
F	*26.75*	*12.99*	*6.0%*
G	*34.98*	*11.37*	*2.8%*

Table 2. Spot lamps half power angles.

The results presented in table 2 reinforce the idea that it is a good approximation to use a generalised Lambertian function model to define the radiation pattern of the analysed spot lamps. The utilisation of such approximation introduces an error which does not exceed *6.0%*. Figure 5 illustrates the curves achieved by this approximation and the corresponding normalised measured values associated to spot lamps A, D, E and F.

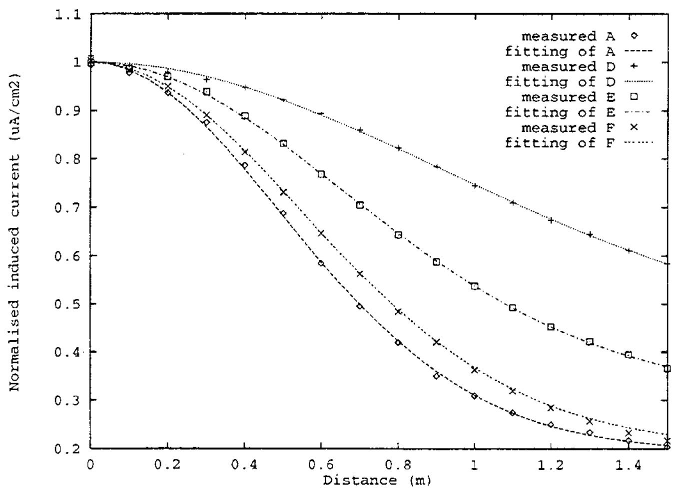

Figure 5. Radiation pattern of spot lamps A, D, E and F.

3.3. Ambient noise model

Usually, the dominant noise in IR wireless communication systems is the ambient light noise which dominates over the receiver noise produced by the electronic components. In [2], it was defined a spatial distributed ambient noise model based on two components: isotropic and directional. The relation between isotropic and directional noise was controlled by a noise ratio parameter (NR) which is defined as the ratio of the directional noise power and the isotropic noise collected at the cell centre by the sectored receiver. The directional noise power contribution from a given noise source is given by a generalised Lambertian function which models a spot lamp. The isotropic noise power contribution is assumed to be collected from a diffusely reflecting surface and is independent of the position of the receiver.

4. PERFORMANCE EVALUATION OF THE OPTICAL SECTORED RECEIVER

4.1. Diversity gain

The SNR in an infrared receiver depends, mainly, of the signal irradiance and of the noise power seen by the receiver photodiode. The diversity gain is defined as the ratio of the worst case SNR of the sectored receiver to the worst-case SNR of a non-sectored reference receiver. The non-sectored reference receiver is an optical receiver oriented vertically with an unitary active area and with a complete *FOV* which means $FOV = 90^o$. The diversity gain of the maximum ratio (MR) sectored receiver over the non-sectored (NS) receiver is given by $G_D = 10 \log (SNR_{MR}) - 10 \log (SNR_{NS})$.

4.2. Discussion and results

Our performance evaluation of optical sectored receivers will follow the analysis presented by Valadas[2]. In our analysis we will consider a maximal-ratio combining method. Sectored receivers will be tested in the default configuration room presented in figure 6 which is a model of test room 2.

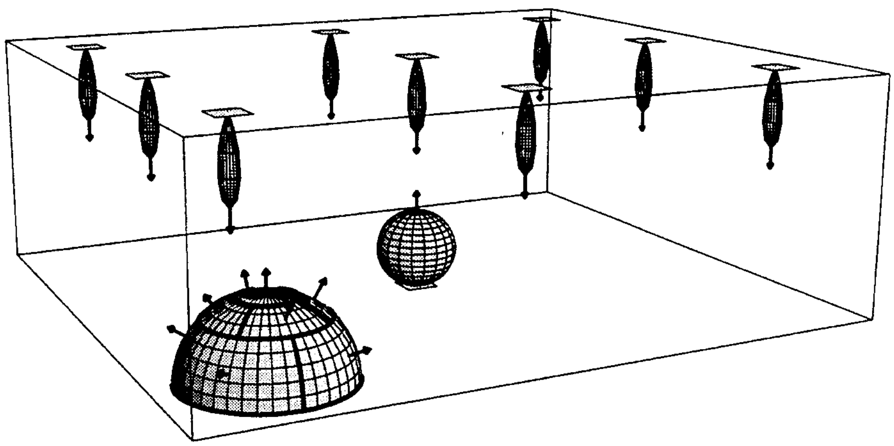

Figure 6. Test room 2 (test room configuration model).

In performance evaluation of the sectored receivers we use the following assumptions: i) there are 9 spot lamps which are assumed Lambertian noise sources with an half power angle of 12.5^o; ii) noise ratio parameter is assumed $NR=10$; iii) the emitter is positioned in the centre of the room and is pointed straight up to the centre of the ceiling, the emitter has an unitary optical power and has an half power angle of 60^o; iv) the reflection coefficient of the ceiling surface is unitary; v) the level of isotropic noise can be calculated at the cell centre from the default value of noise ratio parameter and of the total power emitted by the directional noise sources.

Several sectored receiver configurations were tested. Taking into account the achieved performance, we selected the following four sectored receiver configurations:

Case I:

$$\Psi_I = \{\{ 4, 0^o, 0^o, 30^o\}, \{ 4, 45^o, 30^o, 90^o\}\}$$

Case II:

$$\Psi_{II} = \{\{ 1, 0^o, 0^o, 7.5^o\}, \{ 4, 45^o, 7.5^o, 30^o\}, \{ 4, 0^o, 30^o, 90^o\}\}$$

Case III:

$$\Psi_{III} = \{\{ 5, 0^o, 0^o, 30^o\}, \{ 5, 36^o, 30^o, 90^o\},\}$$

Case IV:

$$\Psi_{IV} = \{\{ 6, 0^o, 0^o, 30^o\}, \{ 6, 30^o, 30^o, 90^o\}\}$$

In a first phase of the performance evaluation we assume a ceiling height of *1.64 m* corresponding to the height from transceiver plane to the ceiling surface. This assumption was taken to ensure that the room configuration model is identical to the environment of test room 2. In our analysis we evaluate the SNR within the default configuration room for the reference receiver and for all sectored receiver configurations. Table 3 shows a summary of the simulation results. It was achieved a SNR improvement of *4.04 dB* to *5.51 dB* by using a sectored receiver instead of a non-sectored receiver. Moreover, the utilisation of sectored receivers equalise the SNR within the communication cell. The SNR dynamic range of a non-sectored receiver is *16.88 dB* while the SNR dynamic range of the four sectored receiver configurations does not exceed *7.86 dB*.

	SNR (*dB*)		**Dynamic Range (*dB*)**	**Diversity Gain (*dB*)**
	Minimum	**Maximum**		
Reference Receiver	*-21.21*	*-4.33*	*16.88*	-
Case I	*-16.83*	*-10.62*	*6.21*	*4.38*
Case II	*-15.70*	*-7.84*	*7.86*	*5.51*
Case III	*-16.98*	*-11.00*	*5.98*	*4.23*
Case IV	*-17.17*	*-11.36*	*5.81*	*4.04*

Table 3. Simulated results using $h = 1.64\ m$.

Figure 7a shows the SNR of the non-sectored receiver as a function of the receiver position within the room. Figure 7b illustrates the SNR of the case II sectored receiver which has the highest diversity gain. As seen in figure 7a, SNR of the non-sectored receiver has its minimum values below the spot lamps. On the other side, the SNR of the case II sectored receiver has its minimum values near the room corners, corresponding to the positions where the signal power has its minimum values and when there is a noise source between the receiver and the emitter.

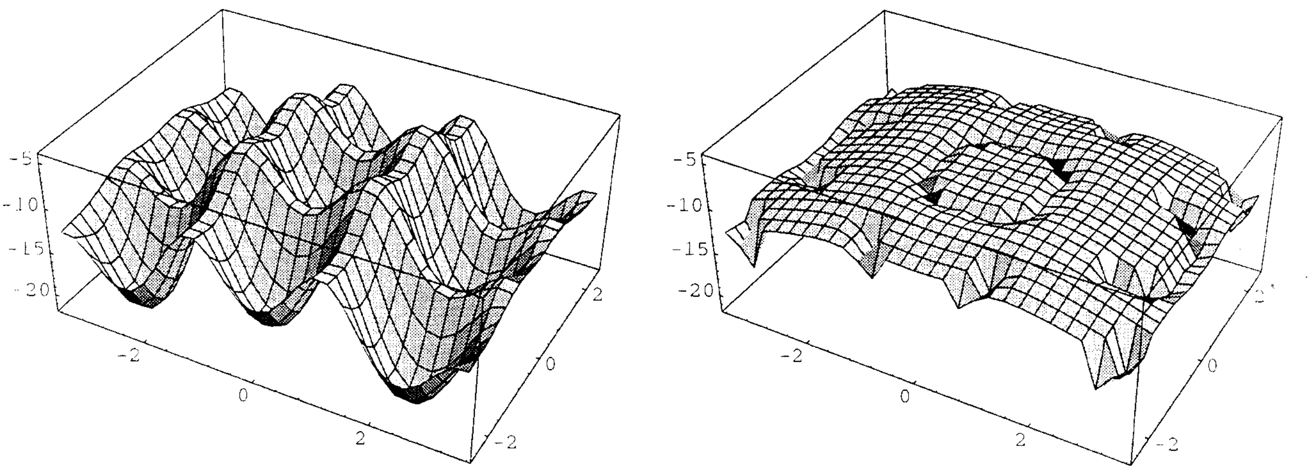

a) **b)**

Figure 7. SNR of the a) non-sectored receiver and b) case II sectored receiver as a function of the receiver position within the room (with $h = 1.64\ m$).

To validate the good performance gains of sectored receivers shown above we extended the performance evaluation of sectored receivers to a higher ceiling room. In this case we consider an hypothetical room with the same area, and the same signal and noise sources of the test room considered above, but with a ceiling height of *3 m* from the receiver to the ceiling. The emitter is placed in the same horizontal plane of the receiver. Here, we evaluate the performance of the same sectored receiver configurations identified by case I, II, III and IV. The simulation results are shown in table 4.

	SNR (*dB*)		Dynamic Range (*dB*)	Diversity Gain (*dB*)
	Minimum	Maximum		
Reference Receiver	*-20.34*	*-14.43*	*5.91*	-
Case I	*-15.41*	*-13.64*	*1.77*	*4.93*
Case II	*-14.67*	*-11.21*	*3.46*	*5.67*
Case III	*-16.41*	*-13.96*	*2.45*	*3.93*
Case IV	*-15.60*	*-14.27*	*1.33*	*4.74*

Table 4. Simulated results using $h = 3.0\ m$.

As seen in table 4, a diversity gain from about *3.93 dB* to about *5.67 dB* was achieved by using an optical sectored receiver instead of a non-sectored receiver. Also, in this situation, the SNR dynamic range of a non-sectored receiver is higher than the SNR dynamic range of any of the considered sectored receivers. Case II sectored receiver has the worst SNR dynamic range and has, once more, the highest diversity gain.

Figures 8a and 8b present the SNR distribution of the non-sectored receiver and of the case II sectored receiver, respectively. Figure 8a shows the minimum SNR of the non-sectored receiver positioned below the spot lamps. This particularity was also observed in the previous situation.

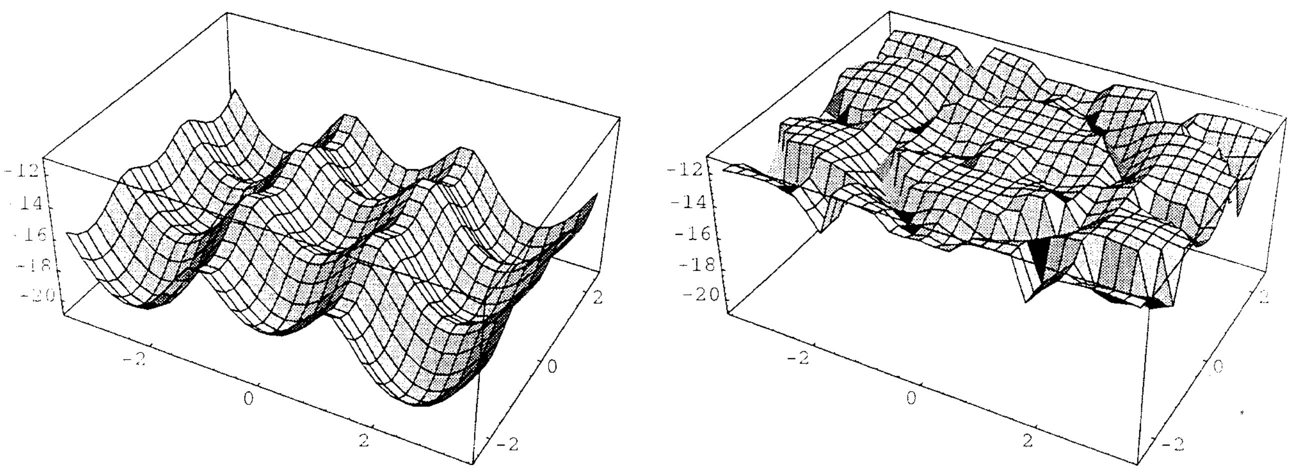

a) b)

Figure 8. SNR of the a) non-sectored receiver and b) case II sectored receiver as a function of the receiver position within the room (with $h = 3.0\ m$).

5. CONCLUSIONS

The good performance of maximum ratio optical sectored receivers was demonstrated in a test room illuminated by 9 directional noise sources. Four sectored receiver configurations were considered and it was shown that significant diversity gains (from *3.93 dB* to *5.67 dB*) were achieved. Moreover, optical sectored receivers presents a SNR dynamic range which is smaller than the SNR dynamic range presented by non-sectored receivers. This means that sectored receivers are less sensitive to the position and orientation and of directional noise sources.

We presented a model for the spot lamp radiation pattern which showed to be a good approximation to the real values. This model was used in the performance evaluation of the sectored receivers. As the following step, it could be interesting to introduce a model of the fluorescent lamps radiation pattern and a model for light noise which emanates from windows.

6. ACKNOWLEDGEMENTS

The first author would like to thanks JNICT (*Junta Nacional de Investigação Científica e Tecnológica*) for its financial support through a Ph.D. grant BD/2599/93. This work was partially funded by the European Commission via project ESPRIT.6892 POWER (*Portable Workstation for Education in Europe*).

7. REFERENCES

1. F. R. Gfeller, U. Bapst, "Wireless In-House Data Communication via Diffuse Infrared Radiation", *Proceedings of the IEEE*, Vol. 67, No. 11, pp. 1474-1486, Nov. 1979.

2. R. T. Valadas, A. M. O. Duarte, "Sectored Receivers for Indoor Wireless Optical Communication Systems", *PIMRC'94, The Fifth IEEE International Symposium on Personal, Indoor and Mobile Radio Communications*, pp. 1090-1095, The Hague, Netherlands, Sep. 18-23, 1994.

3. C. R. A. T. Lomba, R. T. Valadas, A. M. O. Duarte, "Flexible Emitter Radiation Pattern for Indoor Wireless Local Area Networks", *COMCON V, International Conference on Advances in Communication & Control*, Crete, Greece, Jun. 26-30, 1995.

4. J. R. Barry, J. M. Kahn, E. A. Lee, D. G. Messerschmitt, "High-Speed Nondirective Optical Communication for Wireless Networks", *IEEE Network Magazine*, pp. 44-54, Nov. 1991.

5. J. R. Barry, J. M. Kahn, W. J. Krause, E. A. Lee, D. G. Messerschmitt, "Simulation of Multipath Impulse Response for Indoor Wireless Optical Channels", *IEEE Journal on Selected Areas in Communications*, Vol. 11, No. 3, Apr. 1993.

6. C. R. A. T. Lomba, R. T. Valadas, A. M. O. Duarte, "Sectored Receivers to Combat the Multipath Dispersion of the Indoor Optical Channel", *PIMRC'95, The Sixth IEEE International Symposium on Personal, Indoor and Mobile Radio Communications*, Toronto, Canada, Sep. 27-29, 1995.

7. F. R. Gfeller, P. Bernasconi, W. Hirt, C. Elisii, B. Weiss, "Dynamic Cell Planning for Wireless Infrared In-House Data Transmission", *International Zurich Seminar on Digital Communications*, pp. 261-272, Zurich, Switzerland, Mar. 8-11, 1994, Springer-Verlag.

8. A. J. C. Moreira, R. T. Valadas, A. M. O. Duarte, "Artificial Light Interference in Wireless Infrared Transmission Systems", *PIMRC'95, The Sixth IEEE International Symposium on Personal, Indoor and Mobile Radio Communications*, Toronto, Canada, Sep. 27-29, 1995.

9. C. R. A. T. Lomba, R. T. Valadas, A. M. O. Duarte, "Propagation Losses and Impulse Response of the Indoor Optical Channel: A Simulation Package", *International Zurich Seminar on Digital Communications*, pp. 285-297, Zurich, Switzerland, Mar. 8-11, 1994, Springer-Verlag.

10. A. M. R. Tavares, A. J. C. Moreira, C. R. A. T. Lomba, L. M. V. Moreira, R. J. M. T. Valadas, A. M. O. Duarte, "Experimental Results of a 1Mbps IR Transceiver for Indoor Wireless Local Area Networks", *COMCON V, International Conference on Advances in Communication & Control*, Crete, Greece, Jun. 26-30, 1995.